PHYSICAL REVIEW E **75**, 011504 (2007)

Non-Gaussian nature of glassy dynamics by cage to cage motion

Bart Vorselaars,[1,*] Alexey V. Lyulin,[1] K. Karatasos,[2] and M. A. J. Michels[1]
[1]*Group Polymer Physics, Eindhoven Polymer Laboratories and Dutch Polymer Institute, Technische Universiteit Eindhoven, P.O. Box 513, 5600 MB Eindhoven, The Netherlands*
[2]*Chemical Engineering Department, Aristotle Univerisity of Thessaloniki, 54124 Thessaloniki, Greece*
(Received 24 March 2006; revised manuscript received 16 November 2006; published 23 January 2007)

A model based on a single Brownian particle moving in a periodic effective field is used to understand the non-Gaussian dynamics in glassy systems of cage escape and subsequent recaging, often thought to be caused by a heterogeneous glass structure. The results are compared to molecular-dynamics simulations of systems with varying complexity: quasi-two-dimensional colloidlike particles, atactic polystyrene, and a dendritic glass. The model nicely describes generic features of all three topologically different systems, in particular around the maximum of the non-Gaussian parameter. This maximum is a measure for the average distance between cages.

DOI: 10.1103/PhysRevE.75.011504 PACS number(s): 64.70.Pf, 05.40.Fb, 81.05.Kf, 83.10.Mj

I. INTRODUCTION

The most striking feature of glass-forming liquids is a rapid increase of their viscosity when temperature decreases. Usually, the glass-transition temperature is defined as the temperature at which the viscosity reaches 10^{12} Pa s for simple liquids, or at which the intrinsic relaxation time of the material exceeds the experimental time scale. Yet relaxation in liquids and glasses is still an unresolved problem in soft-matter physics [1].

Extensive research has been carried out to study the dynamic *heterogeneity* of the glassy state. Many interpretations exist for this concept of heterogeneous dynamics. A common one is that heterogeneous dynamics is applicable when individual relaxing units have site-specific relaxation times [2]. The size of a relaxing unit is typically a few nm for glasses such as orthoterphenyl [2]. A conventional way to quantify this type of heterogeneity is the observation that the non-Gaussian parameter (NGP) [3]

$$\alpha_2(t) = \frac{\langle \Delta \mathbf{r}(t)^4 \rangle}{(1+2/d)\langle \Delta \mathbf{r}(t)^2 \rangle^2} - 1 \tag{1}$$

is nonzero. Here $\Delta \mathbf{r}(t) = \mathbf{r}(t_0+t) - \mathbf{r}(t_0)$ is the displacement of a particle after a time interval t, d the spatial dimension and $\langle \cdots \rangle$ denotes ensemble averaging. For a system of identical particles described by the diffusion equation, the mean square translational displacement (MSTD) of a particle increases linearly in time, and the van Hove self-correlation function $\langle \delta[\mathbf{R} - \Delta \mathbf{r}(t)] \rangle$ [4] has a Gaussian shape. In this case the NGP is zero. For an ensemble of identical particles in the ballistic regime with a velocity given by the Maxwell-Boltzmann distribution the self-part of the van Hove function is also of a Gaussian shape and the NGP equals zero as well.

It is indeed observed that many simulations of monatomic [3,5,6] and binary systems [7,8], polydisperse liquids [9], metallic glasses [10], salts [11], small molecules [12], glassy networks [13], and polymers [14] do show a nonzero value of the NGP. This behavior is also observed in experiments on colloidlike particles using confocal microscopy [15] and on glassy polymer systems by means of neutron scattering [16]. A particular result is that the NGP peaks at a time t^*, corresponding to the crossover between the so-called cage regime and the diffusive regime of the MSTD. The cage escape is associated with complex dynamic behavior, involving complicated clusters in space and correlated jumps in time. Typical values of the maximum of the NGP range from 0.1 to 10 but higher or lower values have been observed as well.

Nevertheless, the relation between deviations from Gaussian behavior and dynamic heterogeneity in the sense of different relaxation units is not obvious. First note that many causes of non-Gaussian behavior exist, also in glasses. A few possible sources are averaging over intrinsically different types of particles, crossover from ballistic to diffusive motion [17], or anharmonic motion within a cage [16]. The focus of the present study is on non-Gaussian behavior (NGB) occurring close to the glass transition, and related to cage-escape dynamics. Various models are in use, to shed some light on this type of NGB. One of the current models is the well-known mode-coupling theory (MCT) for the glass transition [18]. Yet it predicts a time dependence of $\alpha_2(t)$ which differs significantly from simulation results and, moreover, may strongly underestimate (by about one order of magnitude) the deviations from Gaussian behavior close to the glass transition [8]. The local-mobility model [6] connects the deviations from Gaussian behavior with a fluctuating diffusion coefficient. However, it has the disadvantage that *a priori*, it is not clear to what extent the concept of fluctuating mobilities is reasonable [9]. The trapping-diffusion model of Odagaki *et al.* [19] captures the glassy heterogeneity in a broad relaxation spectrum. It has some communalities with the model of the present study. However, as we will see, a major difference is that it is based on a totally different relaxation spectrum and it predicts that the average relaxation time diverges at the glass transition (as is also the case with the ideal MCT). This is usually not observed both in experiments and in simulations [20]. Yet another model [21] tries to describe non-Gaussian behavior by assuming a wide distribution of jump lengths causing the heterogeneous dynamics. The most probable jump distance is

*Author to whom correspondence should be addressed. Electronic address: b.vorselaars@tue.nl

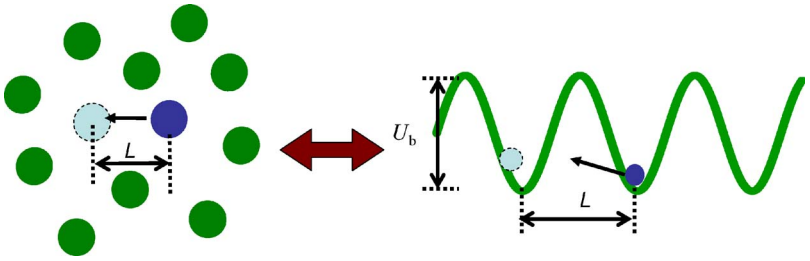

FIG. 1. (Color online) Schematic view of the effective neighborhood model, in which the particle jumps from one cage to another.

then interpreted as a localization length. Each of the last three models assumes some distribution (either in time, jump lengths or diffusion coefficients) to capture a heterogeneous aspect and to explain the non-Gaussian behavior. Still no consensus exists which process is dominating for the non-Gaussian behavior around cage escape and how to quantify this.

The aim of the present study is to employ a simple model for capturing the main physical mechanism underlying the non-Gaussianity of glassy dynamics. The purpose of the model is not to express the glassy dynamics in its full detail (such as aging effects, backscattering, heterogeneity), but only the part which we think is the most relevant for the description of non-Gaussian behavior. In particular it does not assume any heterogeneity in the sense of site-specific relaxation times. The analytical low-temperature results are found to describe quantitatively important features of the NGP acquired by molecular dynamics (MD) simulations of three different kind of systems: a quasi-two-dimensional colloidlike system, atactic polystyrene and a dentritic glass, thereby suggesting that the model describes the main process creating non-Gaussian behavior.

II. MODEL

A particle in a liquid is surrounded by neighbors which hinder its motion, and caging occurs. For example, if the interaction between particles is soft repulsive, the hindered particle needs to overcome an effective energy increase to get closer to the edge of the cage, as it approaches the neighbors. Therefore it is trapped in a local energy minimum. The flanking neighbor particles can lower the increase in energy by moving away and creating more vacancy, or by some other sort of collective rearrangement. After passing the flanking neighbors this particle is again in a local energy minimum if the particle previously at this position experiences a similar type of movement (thereby causing stringlike behavior [22]), or via another cooperative mechanism. So the particle passed an effective energetic barrier. In this new caged position the mechanism repeats itself.

This effect of caging and subsequent cage escape to a new cage can be modeled by the motion of a single particle in an effective field describing the interactions with the neighbor particles in the following way. The particle in question experiences frequent collisions with its neighbors. As the surrounding particles have zero velocity on average, the collision is harder if the velocity of the particle is higher. We describe these two effects by a friction force and a stochastic force acting on the particle. The energy barrier to be passed is modeled by an effective potential. This can be interpreted as a mean-field-like potential. To keep the model simple we restrict ourselves for the moment to the one-dimensional (periodic) sine function. Later on it will be shown that the resulting non-Gaussian parameter does not depend much on the precise shape of this potential, nor on its dimension.

Note that the actual potential is highly fluctuating in space and time, leading to strongly correlated processes at the short time scale. One example of such correlation is that easy local transitions are frequently reversed and repeated, leading to strong back-scattering sequences in the process. Such correlated processes can be resummed in a way as is done in the multiple-scattering theory for transport in disordered media [23,24]. In this picture the atomistic diffusion process can be described quantitatively by a site-to-site hopping process with a large spread in transition probabilities. The resulting mobility, which has a similarity with the diffusion coefficient via the Einstein relation, can then be expressed in terms of effective site-to-site propagation probabilities. These probabilities are then expanded in a multiple-scattering perturbation series involving all other sites. To deal with the correlations the perturbation series is reordered into a renormalized self-avoiding-path expansion, in which closed-loop processes (in particular direct back-scattering events) are fully summed first. After making a closure in the expansion by uncorrelating at a higher level of approximation (e.g., via a T-matrix approximation), one then arrives at a description of the diffusion process on a coarse-grained effective level. When considered at a coarse-grained time scale, the diffusion coefficient contains the local correlated processes, while the effective time constant has the meaning of a dwelling time, i.e., the time after which the probability for a series of repeated local events equals the probability for an escape over a hard local barrier. These hops over a hard barrier have a very small probability of (enhanced) reversal, so that for times above the time scales associated with this process the dynamics can to a good approximation indeed be treated as uncorrelated. The present study is restricted to this coarse-grained picture, with strong back-scattering events resummed. The surrounding cage potential of the particle in question is then also averaged, which justifies the use of the simple sinusoidal.

In the above picture, the dynamics of a particle inside an external field is captured in the Langevin equation (Fig. 1)

$$m\frac{\partial^2 x(t)}{\partial t^2} + \zeta\frac{\partial x(t)}{\partial t} = -\frac{\partial U(x)}{\partial x} + \zeta f(t), \tag{2}$$

with m the mass of the particle, ζ the friction constant, $-\frac{\partial U(x)}{\partial x}$ the force acting on the particle due to the external potential

$U(x)=\frac{1}{2}U_b \sin\left(\frac{2\pi x}{L}\right)$ and $\zeta f(t)$ a random force, of which the first moment is zero and the second moment is $\langle f(t)f(t')\rangle = 2D_0\delta(t-t')$. Here $D_0=\frac{kT}{\zeta}$ is the coarse-grained bare diffusion constant of the particle, U_b the height of the energy barrier, L the (effective) distance between cages and k Boltzmann's constant. Limiting to cases where the inertial term can be neglected, the long-time diffusion coefficient of the particle in the sine potential is given by $D=\frac{L^2}{2d\tau}=D_0\left[I_0\left(\frac{U_b}{2kT}\right)\right]^{-2}$ [25], where I_0 is the modified Bessel function of the first kind and τ is the average time to travel a distance L under the influence of the potential; so τ is of the order of the dwelling time as discussed above.

The non-Gaussian parameter for the dynamics of the particle under the influence of the external potential can be calculated analytically for a sufficiently low temperature-to-barrier ratio, $\frac{kT}{U_b}\ll 1$. In this limit the minimum of the potential can be approximated by a parabola. For very small times the particle is diffusing freely, $\langle \Delta\mathbf{r}(t)^2\rangle = 2dD_0t$. After some time its dynamics is influenced by the potential and the particle becomes trapped; the MSTD reaches a constant value of $\langle \Delta\mathbf{r}(t)^2\rangle = \Delta^2$. Time scales up to the start of caging at $t=t_c=\Delta^2/(2dD_0)$ will be discarded in this calculation. For longer times the particle mostly vibrates in a potential minimum n and due to thermal excitation it occasionally jumps to neighboring minima; the jumping part of the particle motion then obeys the master equation [26]

$$\frac{\partial \Psi_n(t)}{\partial t} = \frac{D}{L^2}[\Psi_{n-1}(t) + \Psi_{n+1}(t) - 2\Psi_n(t)], \tag{3}$$

with $\Psi_n(t)$ the probability that the particle is in a potential well n at time t. It is now straightforward to generalize this one-dimensional random-walk master equation to higher (spatial) dimensions to afford a better comparison to simulation results. Assuming that the MSTD inside a well is of Gaussian nature leads to (see Appendix)

$$\langle \Delta\mathbf{r}(t)^2\rangle = \Delta^2(1 + t/t^*) = \Delta^2 + 2dDt \tag{4}$$

and

$$\langle \Delta\mathbf{r}(t)^4\rangle = (1 + 2/d)\langle \Delta\mathbf{r}(t)^2\rangle^2 + 2dDtL^2, \tag{5}$$

with $t^*=\Delta^2/(2dD)$ and Δ^2 the MSTD within the cage (the plateau value, due to the rattling motion inside the cage). Substituting Eqs. (4) and (5) in Eq. (1) yields the high-effective-barrier result

$$\alpha_2(t) = \frac{L^2}{(1 + 2/d)\Delta^2}\frac{t/t^*}{(1 + t/t^*)^2} = \frac{L^2}{(1 + 2/d)\Delta^2}\frac{2dDt/\Delta^2}{(1 + 2dDt/\Delta^2)^2}, \tag{6}$$

with $d=1$ for the random walk described by Eqs. (2) and (3). Equation (6) in this exact form is also valid for a broader class of random walks, which includes a random walk in random directions, and on regular triangular and cubic lattices (this last case is considered by Odagaki *et al.* [19]); also a distribution of jump lengths results in the same expression (then L represents an effective jump length).

As an additional outcome of the model the fraction of particles which have jumped at least once after some time t can be determined. In the high-effective-barrier limit this fraction is given by $\phi_j(t)=1-\exp\left(-\frac{2dDt}{L^2}\right)$. At t^* this is expressible in terms of the maximum value of the NGP $\phi_j^*=1-\exp\left(-\frac{\Delta^2}{L^2}\right)=1-\exp\{-[4(1+2/d)\alpha_2^*]^{-1}\}$. For a typical value of $\alpha_2^*=2.0$, we have $\phi_j\approx 0.072$, which can be interpreted as the fraction of mobile particles at $t=t^*$.

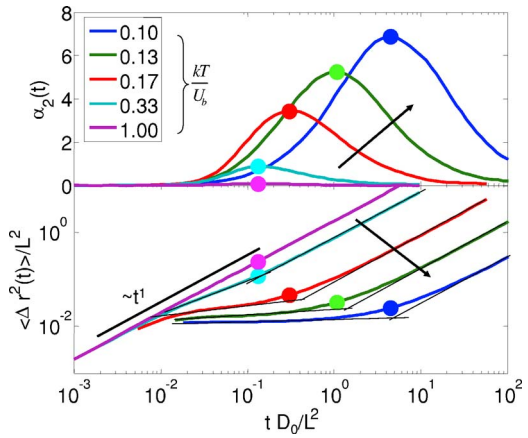

FIG. 2. (Color online) Predictions of the model for the NGP (upper panel) and the MSTD (lower panel) for various $\frac{kT}{U_b}$ ratios. The arrows point towards decreasing ratios. Results are obtained by numerically integrating Eq. (2) [25,27]. The time t^* at which $\alpha_2(t)$ peaks (indicated by bullets) agrees well with the crossover from the cage regime to the final diffusion (intersection of black solid lines).

We summarize our main claims as follows. First of all, a simple one-particle model is suggested which allows an analytical solution for the NGP. In the low temperature-to-barrier case the maximum of $\alpha_2(t)$ is determined by the ratio of the squared jump distance and the value of the MSTD in the cage,

$$\alpha_2^* = \alpha_2(t^*) = \frac{L^2}{4(1 + 2/d)\Delta^2}. \tag{7}$$

Finally, the time at which the NGP peaks, $t=t^*$, is when the rattling part of the MSTD [Δ^2 in Eq. (4)] equals the diffusive part [$2dDt^*$ in Eq. (4)]. For higher ratios of $\frac{kT}{U_b}$, where the plateau region of the MSTD is not that pronounced (see Fig. 2), Eq. (6) is not applicable. In this case the model can be solved numerically and it is still possible to define the crossover time between caged motion and final diffusion as the point at which on a log-log plot for the MSTD vs time the two tangent lines (to the cage regime and to the final diffusive regime) intersect. Again this time is close to t^* (Fig. 2).

III. COMPARISON WITH SIMULATION RESULTS

We compare the predictions of the model to results from simulations of three distinctly different glassy systems. The quasi-two-dimensional colloidlike monatomic system simulated by Zangi and Rice [5] shows NGB. Here particles of diameter σ are confined to a slab with a width $W=1.2\sigma$ and interact with each other via a purely repulsive potential. Simulation results of Ref. [5] for the in-plane MSTD and NGP are fitted with the model for various number densities ρ

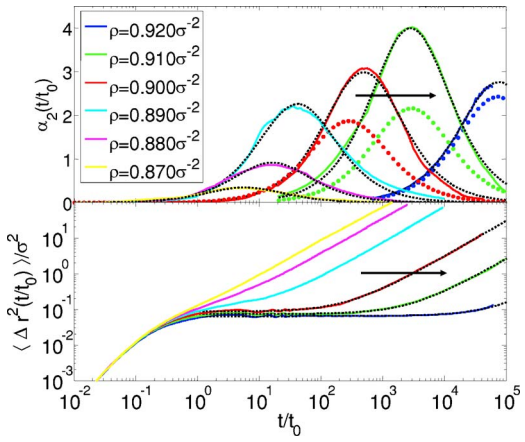

FIG. 3. (Color online) Predictions of the model and simulation results for the colloidlike system [5] for various densities ρ, for the NGP and MSTD parallel to the slab. The arrows point towards increasing densities. Here t_0 is the unit of time [5]. Black lines (small dots) are fits of the model [MSTD, Eq. (4); NGP, Eq. (6)] to the simulation results (solid colored lines). The colored lines (large dots) for the NGP are predictions of the model by an independent set of parameters, see main text.

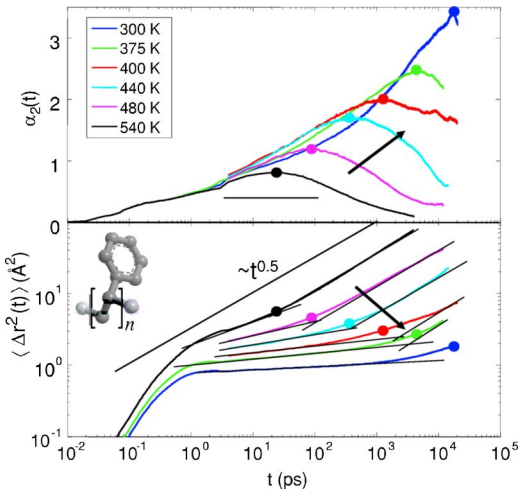

FIG. 4. (Color online) NPG and MSTD of atactic polystyrene (shown is the monomer unit) for various temperatures. The arrows point towards decreasing temperatures. The MSTD crossover time from caging to Rouse diffusion [$\langle \Delta \mathbf{r}(t)^2 \rangle \sim t^{0.5}$ [27]] is close to the time at which $\alpha_2(t)$ peaks. The horizontal bar indicates the FWHM of the NGP for a time-independent diffusion coefficient (see text).

in two ways. First we use Eq. (6) and treat $t^* = \Delta^2/(2dD)$ and the ratio L^2/Δ^2 as two adjustable parameters. In this case the full shape of the NGP is reproduced remarkably well (see the full colored lines vs black dotted lines in Fig. 3), especially for high densities (i.e., high effective barriers). Note that the analytical expression for the NGP, Eq. (6), implies that its full-width at half-maximum (FWHM) on a log scale is not adjustable but has the constant value of $w = \log_{10}(t_{\text{high}}/t_{\text{low}}) = \log_{10}(17+12\sqrt{2}) \approx 1.53$. Nevertheless it adequately describes the simulation results, $w = 1.43$ and 1.48 at $\rho = 0.900\sigma^{-2}$ and $0.910\sigma^{-2}$, respectively.

Alternatively, we can find the values of the model parameters for the NGP in an independent way, namely from the MSTD together with an estimate of the cage to cage distance. Fitting the simulated MSTD for the densities for which there exists a definite plateau [$\langle \Delta \mathbf{r}(t)^2 \rangle \sim t^0$] with Eq. (4) renders the plateau value Δ^2 and a prediction for t^*. To determine the maximum value of the NGP, α_2^*, the effective jump-length L is needed as well. Presuming that it corresponds to the distance between the nearest neighbors, L is calculated by assuming that the particles are placed on a triangular lattice, so that $L^{-2} = \frac{\sqrt{3}}{2}\rho$.

Two distinct aspects are observed, when comparing this alternative fit to the simulation results (compare solid vs large-dotted colored lines, Fig. 3). First, it can be seen that the cage-diffusion crossover time in the MSTD is equal to the time at which the NGP peaks, t^*, in accordance with the prediction of the model. Second, this parameter-free fit underestimates the maximum of the NGP by at most a factor of 2.

A higher peak value of the NGP can be interpreted as being due to a larger effective jump length than the nearest-neighbor distance. This suggests that also next-nearest-neighbor jumps as well as jumps of higher order could be important. It can be shown that when one takes into account these multiple jump lengths, only the effective jump length L of Eq. (6) changes, while the functional form of $\alpha_2(t)$ remains invariant. Nevertheless, it seems that for the highest density this multiple-jump-length effect vanishes and the accordance with the model is better when assuming a single jump length.

In order to study polymer-specific effects of the non-Gaussian dynamics we have performed molecular-dynamics simulations of a melt of atactic polystyrene (PS), one of the most common polymer glass formers. Simulation details are in Ref. [28]. The glass-transition temperature T_g for the PS melt of eight chains of 80 monomers each is around 370 K. The MSTD and the NGP, after averaging over all united atoms, are shown in Fig. 4.

Some generic features of the one-particle model can also be seen for this polymer system. The peak time of the NGP, t^* is also situated at the crossover from the cage regime to Rouse-like diffusion. However, because of the different bonded interactions of the backbone and the phenyl-ring atoms, the jump distances, the cage sizes and the mobilities of these atoms are different as well. We therefore compare only the values of the MSTD and NGP for atoms in the backbone (including the first atom of the phenyl ring and excluding chain ends). We assume that the jump distance is now due to an internal torsion potential in the polymer chain; this potential favors specific positions of the atoms, corresponding to *trans* or *gauche* conformations. We also assume that these conformations are separated by a distance L between them of about 2.5 Å. At $T = 375$ K the plateau value of the MSTD is $\Delta^2 \approx 0.64$ Å^2. Using Eq. (7) with these values of Δ^2 and L gives then $\alpha_2^* = 1.5$, which is remarkably close to the simulated value $\alpha_2^* = 1.3$.

The molecular-dynamics simulations also show that the shape of the NGP is similar to but much wider than the prediction of the one-particle model. The FWHM in case of a time-independent diffusion coefficient is shown in Fig. 4 as

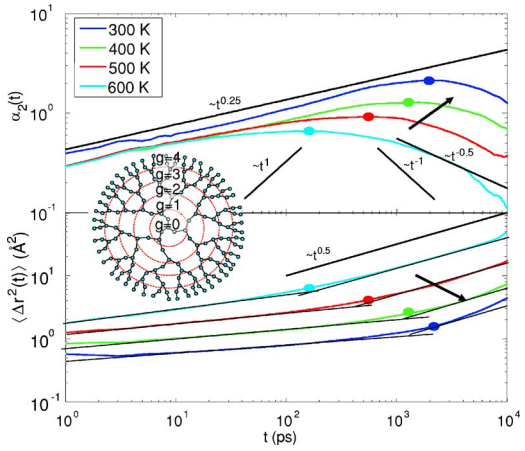

FIG. 5. (Color online) Same as Fig. 4, but for the dendrimer melt, of which the architecture is shown.

a bar. This difference can be partly explained by the anomalous (nonlinear in time) Rouse diffusion of the segments in a polymer chain, $\langle \Delta \mathbf{r}(t)^2 \rangle \sim t^{1/2}$. Note that for a time-independent diffusion coefficient, a result of the model is that the NGP increases linearly in time for $t_c < t < t^*$, i.e., $\alpha_2(t) \sim t^1$ [Eq. (6)]. A broader peak can be interpreted in terms of a lower effective scaling exponent of the NGP for $t_c < t < t^*$. Using the Rouse exponent 1/2 (so $D \sim t^{-1/2}$) in Eq. (6) indeed results in a broader peak. Still, this anomalous diffusion cannot fully explain the broad shape of $\alpha_2(t)$ occurring with polystyrene (Fig. 4). It is possible that due to disorder in the polymer structure close to the glass transition the packing is not ideal, and a varying environment is present. As a result low-energy pathways are preferential and single-file diffusion is enhanced. It is known that this type of diffusion is anomalous as well, $\langle \Delta \mathbf{r}(t)^2 \rangle \sim t^{1/2}$ [29]. The combination of Rouse-like and single-file diffusion (giving an effective exponent of 1/4 for $t < t^*$) could be the cause for this wider peak. Another possible cause is that the various united atoms are not identical, due to the different bonded interactions. This results in different dynamics and thereby promotes a wider relaxation distribution.

Finally, we have performed molecular-dynamics simulations of a perfectly branched dendritic melt (see Ref. [30] for details). The atom connectivity of this system has an even more complex structure than in the previous case. In the present study we only show results for the fourth-generation dendrimer melt, for which the glass transition occurs around $T_g = 500$ K, although results for other generations are similar. The MSTD and the NGP of the outer-generation atoms are given in Fig. 5. As with the PS glass, the same main features of the model are observed for this system. Following the same analysis as for the polymer glass, the prediction of the model for $T = 500$ K (assuming a *trans-gauche* distance of 2.5 Å as the most dominant jump-length L and using the plateau value of the MSTD, $\Delta^2 = 1.25$ Å^2) is $\alpha_2^* = 0.75$, compared to the simulation result of $\alpha_2^* = 0.92$. This similarity appears to indicate that the model indeed captures the dominant mechanism responsible for non-Gaussian behavior. Similar to the PS melt, the simulated NGP is broader than the calculated one. We assume that a similar reasoning as for the polystyrene system (Rouse-alike and single-file dynamics) may be applied here as well to account for the extra broadening.

IV. SUMMARY AND CONCLUSIONS

In short, we have shown that some universal aspects of the non-Gaussian dynamics (observed for many systems [5–16]) around the cage-diffusion transition can well be explained by a simple model, which does not assume *a priori* any heterogeneity of glassy dynamics (in the sense as mentioned in the introduction). For this model the maximum of the NGP occurs at the crossover between the caged plateau and the final diffusion and the maximal height of the NGP is given by Eq. (7). These statements are confirmed even within fair quantitative detail by simulation results for glass-forming systems with widely different topology—a quasi-two-dimensional colloidlike low-molecular-weight glass former, linear polystyrene glass, and a glass of perfectly branched dendrimers. It is important to emphasize that this model considers the motion at a coarse-grained time scale. It only assumes the existence of cages in which the cage to cage motion results in non-Gaussian behavior. No further details of any explicit collective or heterogeneous glassy dynamics are required to understand the non-Gaussian behavior in this sense.

In contrast to the low-molecular weight liquids, additional intrachain (torsional) interactions in polymer melts make multiple jumps very unlikely, and the predictions of the model regarding the maximum of the NGP are found to be closer to the simulated results. On the other hand, the polymer connectivity introduces more complicated anomalous diffusion effects, which effectively broadens the simulated NGP peak.

ACKNOWLEDGMENTS

The authors are grateful to R. Zangi and S. A. Rice for kindly providing their simulation results for the colloidlike system. K. K. acknowledges funding from the Greek General Secretariat for Research and Technology under the framework of the PENED 2003 Program (Grant No. 03ED716).

APPENDIX: RANDOM WALK

We will show in this Appendix how one can determine the expressions for the mean-square translational displacement and the mean quartic translational displacement for a certain class of random walks [i.e., Eqs. (4) and (5)]. First we will look at a discrete random walk, in which the particle makes a jump after each step i in some direction $\mathbf{x}_i$ with a certain probability distribution for the step vector $\rho(\mathbf{x}_i)$. Later on the time dependency is introduced.

We only consider random walks for which $\rho(\mathbf{L}) = \rho(-\mathbf{L})$, i.e., a walk of Pólya type (Ref. [31], Sec. I.3.3). Then the MSTD for a n-step random walk is $\langle \Delta \mathbf{r}(n)^2 \rangle = nL^2$, with $\Delta \mathbf{r}(n) = \Sigma_{i=1}^n \mathbf{x}_i$, $L^2 = \langle \mathbf{x}_i \cdot \mathbf{x}_i \rangle = \langle \mathbf{x}_i^2 \rangle$ (Ref. [31], Sec. I.2.1) and $\langle \cdots \rangle$ denoting averaging over all possible step vectors.

The discrete mean quartic translational displacement (MQTD) is then

$$\langle \Delta \mathbf{r}(n)^4 \rangle = \sum_i \sum_j \sum_k \sum_l \langle (\mathbf{x}_i \cdot \mathbf{x}_j)(\mathbf{x}_k \cdot \mathbf{x}_l) \rangle. \tag{A1}$$

One can easily see that the only terms in the right-hand side of Eq. (A1) which do not cancel to zero when averaging over all possible steps $\mathbf{L}$ are when $i=j=k=l$ (n terms), $i=j\neq k=l$, $i=k\neq j=l$ and $i=l\neq j=k$ [all $n(n-1)$ terms]. Therefore the discrete MQTD is

$$\langle \Delta \mathbf{r}(n)^4 \rangle = n\langle \mathbf{x}_i^4 \rangle + n(n-1)L^4 + 2n(n-1)\langle (\mathbf{x}_i \cdot \mathbf{x}_j)^2 \rangle.$$

The time-dependent MSTD (and MQTD) is then acquired by observing that the chance for n jumps at time t is described by the Poisson distribution $\rho_n(t)=\exp(-t/\tau)\frac{(t/\tau)^n}{n!}$. Here τ is the average time it takes to make a jump. It is assumed that nonjumped particles already have a constant value of the MSTD Δ^2 within the cage. Then the time-dependent MSTD is

$$\langle \Delta \mathbf{r}(t)^2 \rangle = \Delta^2 + \exp(-t/\tau)\sum_{n=0}^{\infty} \frac{(t/\tau)^n}{n!}\langle \Delta \mathbf{r}(n)^2 \rangle = \Delta^2 + L^2 t/\tau.$$

We will further limit ourselves to random walks in which all steps are of equal length, $|\mathbf{x}_i|=L$ (so $\langle \mathbf{x}_i^4 \rangle = L^4$); and obeys $\langle (\mathbf{x}_i \cdot \mathbf{x}_j)^2 \rangle = L^4/d$. Random walks adhering to these two conditions are, for example, a d-dimensional random flight, a two-dimensional triangular, a three-dimensional body-centered-cubic, and a three-dimensional face-centered-cubic lattice. These relations can be checked for each type of random walk by straightforward calculations (i.e., averaging over all possible step vectors). Repeating the calculation for the time-dependent MQTD and assuming that the displacement within the cage obeys Gaussian statistics [i.e., $\Delta^4=(1+2/d)(\Delta^2)^2$] results in

$$\langle \Delta \mathbf{r}(t)^4 \rangle = (1+2/d)\langle \Delta \mathbf{r}(t)^2 \rangle^2 + L^4 t/\tau,$$

which completes the determination of the two moments.

[1] M. Ediger, C. Angell, and S. R. Nagel, J. Phys. Chem. **100**, 13200 (1996).
[2] R. Richert, J. Phys.: Condens. Matter **14**, R703 (2002).
[3] A. Rahman, Phys. Rev. **136**, A405 (1964).
[4] L. van Hove, Phys. Rev. **95**, 249 (1954).
[5] R. Zangi and S. A. Rice, Phys. Rev. Lett. **92**, 035502 (2004).
[6] M. Hurley and P. Harrowell, J. Chem. Phys. **105**, 10521 (1996).
[7] W. Kob and H. C. Andersen, Phys. Rev. E **51**, 4626 (1995).
[8] E. Flenner and G. Szamel, Phys. Rev. E **72**, 031508 (2005).
[9] B. Doliwa and A. Heuer, J. Phys.: Condens. Matter **11**, A277 (1999).
[10] M. Kluge and H. R. Schober, Phys. Rev. B **70**, 224209 (2004).
[11] S. Itoh, Y. Hiwatari, and H. Miyagawa, J. Non-Cryst. Solids **156**, 559 (1993).
[12] F. Sciortino, P. Gallo, P. Tartaglia, and S. H. Chen, Phys. Rev. E **54**, 6331 (1996).
[13] J. Horbach, W. Kob, and K. Binder, Philos. Mag. B **77**, 297 (1998).
[14] R.-J. Roe, J. Chem. Phys. **100**, 1610 (1994).
[15] E. R. Weeks and D. A. Weitz, Phys. Rev. Lett. **89**, 095704 (2002).
[16] R. Zorn, Phys. Rev. B **55**, 6249 (1997).
[17] R. C. Desai, J. Chem. Phys. **44**, 77 (1966).
[18] M. Fuchs, W. Götze, and M. R. Mayr, Phys. Rev. E **58**, 3384 (1998); C. Kaur and S. P. Das, Phys. Rev. Lett. **89**, 085701 (2002).
[19] T. Odagaki and Y. Hiwatari, Phys. Rev. A **43**, 1103 (1991).
[20] Pablo G. Debenedetti, *Metastable Liquids—Concepts and Principles* (Princeton University Press, Princeton, NJ, 1996).
[21] A. Arbe, J. Colmenero, F. Alvarez, M. Monkenbusch, D. Richter, B. Farago, and B. Frick, Phys. Rev. E **67**, 051802 (2003).
[22] C. Donati, J. F. Douglas, W. Kob, S. J. Plimpton, P. H. Poole, and S. C. Glotzer, Phys. Rev. Lett. **80**, 2338 (1998).
[23] See, e.g., M. P. J. van Staveren, H. B. Brom, and L. J. de Jongh, Phys. Rep. **208**, 1 (1991).
[24] B. Movaghar and W. Schirmacher, J. Phys. C **14**, 859 (1981).
[25] H. Risken, *The Fokker-Planck Equation—Methods of Solution and Applications*, 2nd ed. (Springer-Verlag, Berlin, 1989).
[26] N. G. v. Kampen, *Stochastic Processes in Physics and Chemistry* (North-Holland, Amsterdam, 1981).
[27] M. Doi, *Introduction to Polymer Physics* (Oxford University Press, Oxford, Great Britain, 1995).
[28] A. V. Lyulin, N. K. Balabaev, and M. Michels, Macromolecules **35**, 9595 (2002).
[29] P. M. Richards, Phys. Rev. B **16**, 1393 (1977).
[30] K. Karatasos, Macromolecules **38**, 4472 (2005).
[31] B. D. Hughes, *Random Walks and Random Environments* (Clarendon, Oxford University Press, Oxford, New York, 1995).